Environ Earth Sci (2017) 76:170
DOI 10.1007/s12665-017-6498-8

ORIGINAL ARTICLE

Assessing cave internal aerology in understanding carbon dioxide (CO_2) dynamics: implications on calcite mass variation on the wall of Lascaux Cave (France)

N. Houillon[1] · R. Lastennet[1] · A. Denis[1] · P. Malaurent[1] · S. Minvielle[1] · N. Peyraube[1]

Received: 15 July 2016 / Accepted: 11 February 2017

Abstract Carbon dioxide gas is a key component in dissolution and precipitation of carbonates in karst and cave systems. Therefore, characterizing the internal aerology of a cave is essential to obtain the spatiotemporal distribution of temperature and CO_2 level. In this research, Lascaux Cave (France), an important adorned cavity, was studied. First, the spatiotemporal distribution of CO_2 and temperatures were examined using continuous monitoring at a per minute basis. High-resolution spatial measurements (14 PCO_2 locations and 27 locations for temperature) were carried out for a year in the epikarst and the cave (February 2015 to February 2016). The spatiotemporal analysis presents that air and rock temperatures vary for less than a degree Celsius (12.4–12.9 °C). These are controlled by the conduction of the external thermal waves through the overlying calcarenite massif. As a consequence, two seasonal internal aerologic regimes were identified: stratification and convection. These regimes govern the spatiotemporal distribution of the CO_2 levels (1.1–3.7%), showing that this parameter is a good natural marker of the internal air movements. Second, a method was proposed to estimate the calcite mass potentially affected by condensation water (dissolution process) and exfiltration water (precipitation process). This method, based on numerical simulations, relies on CO_2 and air and rock temperature spatiotemporal distributions in the cave. Third, the method was applied using the case of the left wall of the Hall of the Bulls (one of the most adorned part of the cave). Results showed that the calcite mass, possibly dissolved, varies from 0.0002 to 0.006 g when the mass potentially precipitated is higher (from 0.013 to 0.067 g) depending on the aerologic conditions. This method allows determining which alteration process (e.g., precipitation or dissolution) could eventually lead to the largest variation of calcite on the wall. The results can serve as useful data to the cave experts of the French Ministry of Culture and Communication in terms of Lascaux Cave management policies.

Keywords Carbon dioxide · Complex monitoring · Karst cave aerology · Calcium carbonate

Introduction

Carbon dioxide (CO_2) is involved in the processes that affect calcite in karst cavities (White 1988). This gas increases the dissolution capacity of condensation water and, potentially, of the exfiltration water. On the contrary, decrease in the partial pressure of CO_2 (PCO_2) in the cavity can augment degassing of exfiltration water and calcite precipitation. Hence, it is an important parameter in studying the speleothems (Spötl et al. 2005; Scholz et al. 2009; Dreybrodt and Scholz 2011; Breecker 2017) and in considering the conservation concerns of adorned caves (Fernandez et al. 1986; Cigna 2002). This water is loaded of dissolved CO_2 after flowing in the soil and the epikarst. CO_2 is produced in the subsurface layer by organic matter degradation and root respiration (Kuzyakov 2006). The average CO_2 partial pressure in the Earth's atmosphere is about 0.0407% (NOAA, ESRL Global Monitoring Division (2016), measurements performed at Mace Head site, Ireland). This gas accumulates in the pores and the fissures or cracks in the vadose zone (Bourges et al. 2012). Benavente et al. (2010) measured a

✉ N. Houillon
nicolas.houillon@u-bordeaux.fr

[1] Laboratory I2M-GCE (UMR 5295), University of Bordeaux, Allée Geoffroy Saint Hilaire, Pessac Cédex 33615, France

Published online: 18 February 2017

high-value PCO_2 of about of 6% in the vadose zone of Nerja Cave (Spain). This gas transfers to the cavity in a gaseous or dissolved form (Kaufmann and Dreybrodt 2007). The atmosphere of some cavities, therefore, presents significant PCO_2 levels: 3.4% in the Chauvet Cave (Mangin et al. 1999), 2% in Aven d'Orgnac (Bourges et al. 2006) and about 6% in the Grandes Combes Cave (Batiot-Guilhe et al. 2007).

Several CO_2 studies have been conducted for varying objectives. Some studies aimed to understand the dynamics of CO_2 in the cavities in relation to their external environment (Renault 1968; James 1977; Ek 1981; Troester and White 1984). The spatiotemporal distribution of CO_2 in karst cavities was studied in the past (Atkinson 1977; Wood and Petraitis 1984; Ek and Gewelt 1985; Wood 1985; Batiot 2002). Lately, Baldini et al. (2006), Milanolo and Gabrovšek (2009) and Fernandez-Cortes et al. (2015) showed high-resolution maps of CO_2 distribution to identify CO_2 sources and sinks in the karst cavities. Researchers presented the daily and seasonal CO_2 variations in cavities (Liñán et al. 2008; Kowalski et al. 2008; Kowalczk 2009; Kowalczk and Froelich 2010; Cuezva et al. 2011; Garcia-Anton et al. 2014; McDonough et al. 2016; Vieten et al. 2016). These variations gave light to the cave blowing and inhaling effects due to the interaction of the external atmosphere and cave air (Peyraube et al. 2016). However, none of these studies are based on an in situ high-resolution and high-frequency monitoring similar to the operational activities present in Lascaux Cave.

Lascaux Cave is famous for its engravings and most especially its paintings (Aujoulat 2004; Delluc and Delluc 2006). In fact, this is one of the adorned caves that have the most number of paintings from the Paleolithic age (16,000–17,000 years ago). This cave was discovered in 1940 and was allowed to be visited only until 1963. Since 1979, this cave is classified as one of the UNESCO World Heritage sites. It is only accessible to scientific studies and cave conservation activities. In line with the conservation measures of this important heritage, continuous monitoring of CO_2 and temperature are put in place. This led to detailed observations of the different processes that can affect the walls of this adorned cave such as condensation or wall cavity drying as well as variations in CO_2 level in each part of the cavity.

Understanding the mechanisms responsible to the dynamic equilibrium of the cave is complex as it is still evolving. Cave monitoring since 1963 showed that the air is condensing on the wall for about 6 months per year. This phenomenon is triggered by the changing temperature of the rock surface and in the cave air. This can result in condensation and, consequently, to calcium carbonate dissolution because of the presence of high CO_2 level. At the same time, water exfiltration present in the stratigraphic boundaries of some walls of the cavity is susceptible to calcium carbonate precipitation on the wall. This precipitation depends on the thermodynamic equilibrium of the cavity conditions (temperature, CO_2, etc.) and the geochemical signal of water.

For these reasons, it is found important to understand the dynamics of the cave air or its internal aerology to explain the spatiotemporal distribution of CO_2. In order to do so, high-frequency monitoring with high data resolution from the microclimatic parameters is conducted. Measurements of the CO_2 concentration in the epikarst, the upper weathered layer of rock beneath the soil above the transmission zone (Williams 1983) and geochemical monitoring of an epikarstic emergence located at the entrance of the cave are also carried out. These measurements were used to constrain the geochemistry of water exfiltration. Maps are provided projecting the interpolated CO_2 concentrations based on in situ monitoring done during different periods of the year. A model using simulations obtained from PHREEQC (USGS) was employed to estimate the calcite mass, potentially dissolved or precipitated depending on the PCO_2 and temperature condition. This is to present the influence of the internal aerology of the karst cavity, specifically, on the dissolution and calcite precipitation on the wall through condensation and exfiltration waters. An application of the method in one of the adorned walls of the cave (the left wall of the Hall of the Bulls) was presented. Each estimation of the potential mass of the calcite, however, considered a given PCO_2 and temperature. Assessments on the evolution of the calcite mass and mass balance are beyond the reach of this study.

Site background: geological and geomorphological description

Geological and climatic background

Lascaux Cave is located in the northeast edge of the Aquitaine Basin in Dordogne 200 km east of Bordeaux (Fig. 1). The hill of Lascaux is a promontory of the Upper Cretaceous calcarenite. It is bordered to the west by the Vézère river valley which constitutes the local base level.

The climate of Dordogne is predominantly oceanic with some continental influences as showed by having occasional snow during the winter months. Average rainfall rate is about 880 mm per year. Precipitation is distributed in three main seasons of the year: autumn, winter and spring. Air temperature, on the average, at the site of Lascaux is about 12.6 °C, with monthly temperature fluctuating between 3 °C in winter and 23 °C in summer.

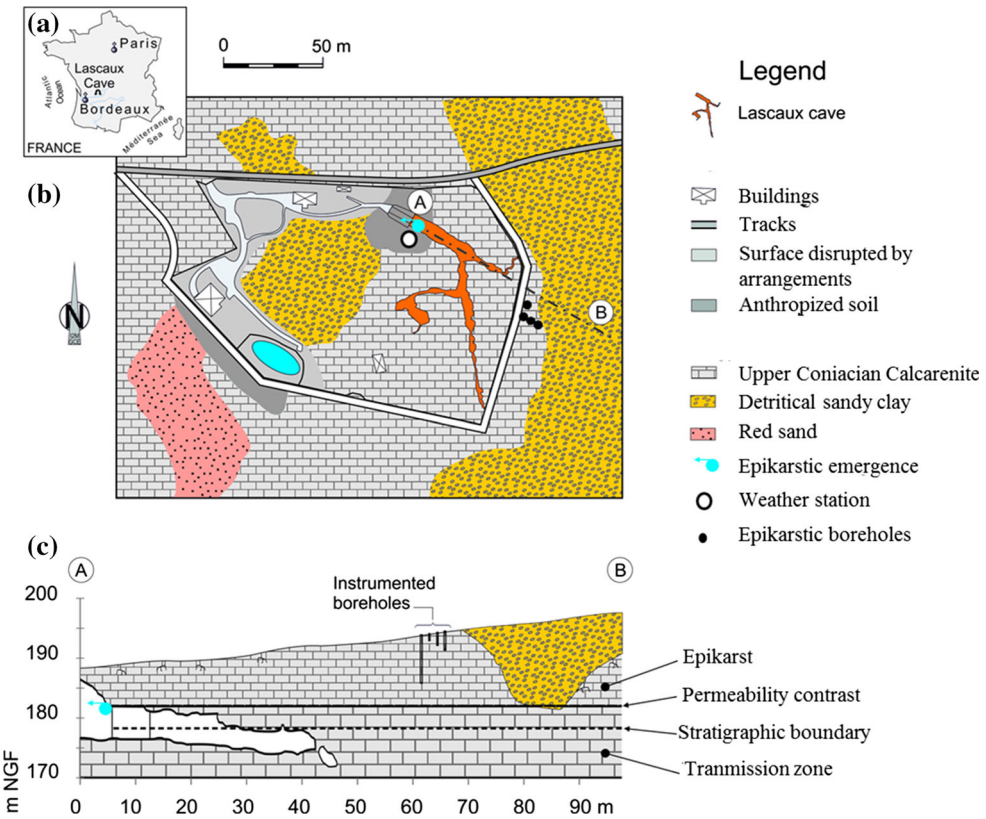

Fig. 1 Location of the Lascaux Cave in the northeast edge of the Aquitaine basin (**a**), in the city of Montignac (Dordogne, France). Geological map of the sedimentary formations constituting the karstic system of Lascaux (**b**). Simplified geological cross section of the cave and its geological environment (**c**). Four boreholes equipped for monitoring the epikarstic air PCO_2 and the weather station locations are presented

With regard to the geological background (Fig. 1a), the hill of Lascaux is mostly constituted of a thick succession of Coniacian calcarenite in which the karstic network including Lascaux Cave is developed. The site of Lascaux is characterized by a remarkable geomorphology comprised of calcarenite projection notched by depressions of around 20 m deep. These depressions are filled by detrital sandy clay formation and red sand. In terms of hydrogeological background, Lascaux Cave is situated in a karstic system still home to water flow of different types. First, an epikarstic emergence is located at shallow depth (6 m) in the airlock of the cave (the SAS1 spring). This part of the cave intersects the interface between the fractured calcarenite of the epikarst and the transmission zone composed of more massive calcarenite layers. These epikarstic flows usually begin in late autumn (November) and end in late spring (June). At present, it is collected in the airlock (SAS1) and evacuated out of the cave. In addition, there is also water exfiltration recorded in the stratigraphic boundary at the interface of the calcarenite layers of the Hall of the Bulls' walls. Exfiltration usually occurs between June and November with a three-month delay compared to the beginning of the epikarstic flows. This exfiltration is assumed to come from the same origin of the epikarstic flows. However, this exfiltration represents a smaller discharge (measurements logistically impossible).

Cave geomorphology description

Lascaux Cave is developed in the unsaturated zone of a karstic system at shallow depths (from 0 to 25 m depth). Its only entrance is isolated from the exterior atmosphere by a steel door and two airlocks (SAS1 and SAS2) to ensure the climatological stability of the cave. The cave is 250 m long (all rooms counted), presenting a vertical drop of 25 m. It is usually divided in three parts: the axial one, the right one and the Great Fissure. Figures 2 and 3 provide a complete schematic map, on the overview, of the cave and a three-dimensional representation of the cave according to the three-dimensional survey of the cavity. The first part corresponds to the Hall of the Bulls and the Axial Gallery. This represents the most known and numbered painted zone in the cave. It is formed by a 35-m-long and 6-m-wide conduit in the Hall of the Bulls and 2 m wide in the Axial Gallery with a significant constriction in the middle of this channel. A perpendicular 15-m-long and winding umbilical conduit extends to the end of the Axial Gallery.

The right part of the cave consists of an 80-m-long conduit starting on the right side of the Hall of the Bulls. This conduit is almost flat in its first part named Passageway which represents an exchange zone between the upper (axial part) and the lower part (right part and the Great Fissure) of the cavity as indicated by alteration zones. It

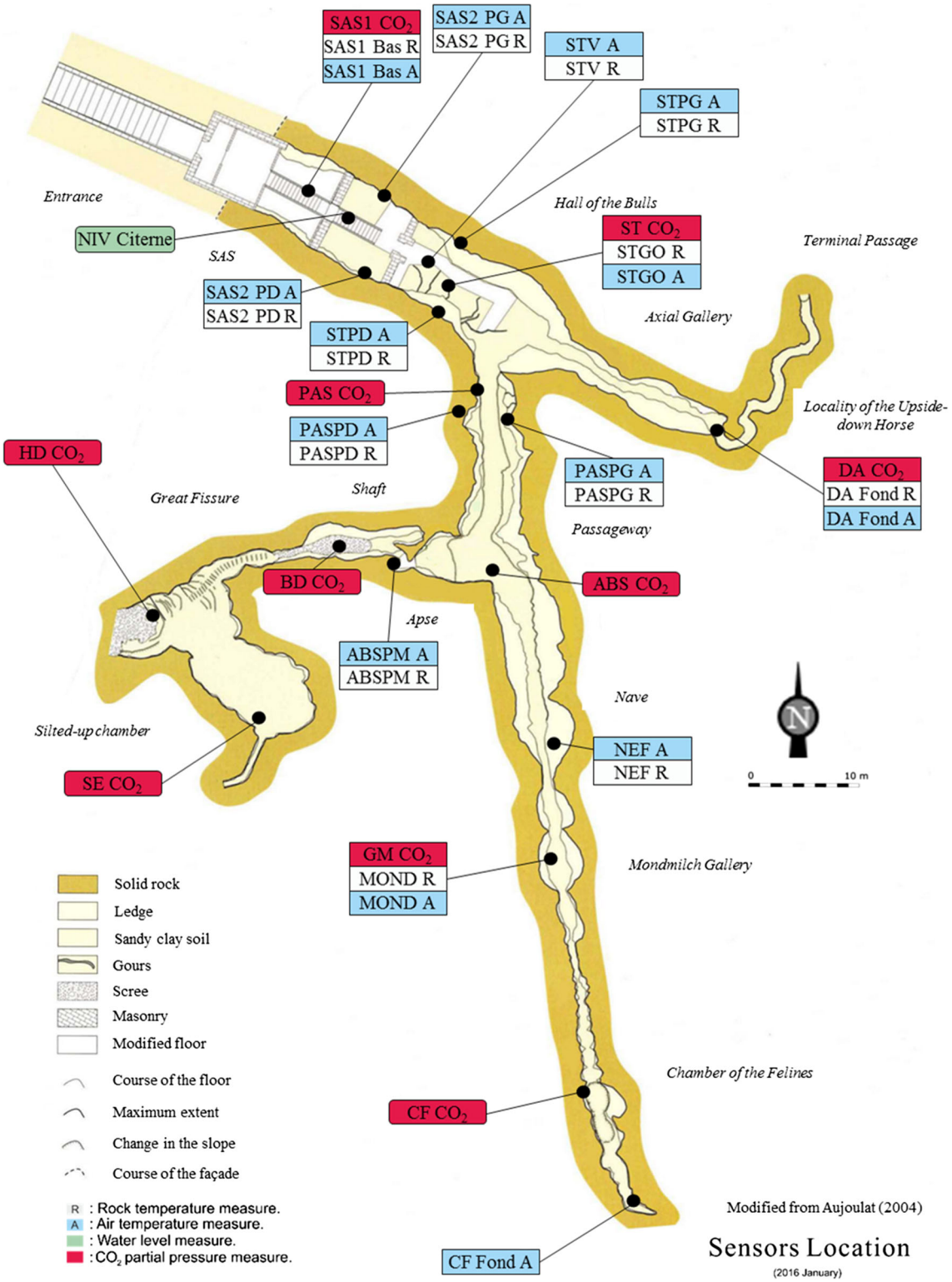

Fig. 2 Schematic plan view of the Lascaux Cave with locations of the different rooms and of the different sensors of interest constituting the continuous monitoring system. Sensors denominations are concordant with the Lascaux rooms historical name (modified from Aujoulat 2004)

opens in the Apse, a 4-m-high circular zone. From the south of this zone, starts the end of the conduit with the Nave, the Mondmilch Gallery and the Chamber of the Felines. Nave is a 20-m-long and 5-m-wide corridor in which the vault is more than 5 m high. This part of the cave presents a 6-m vertical drop. This segment is extended by

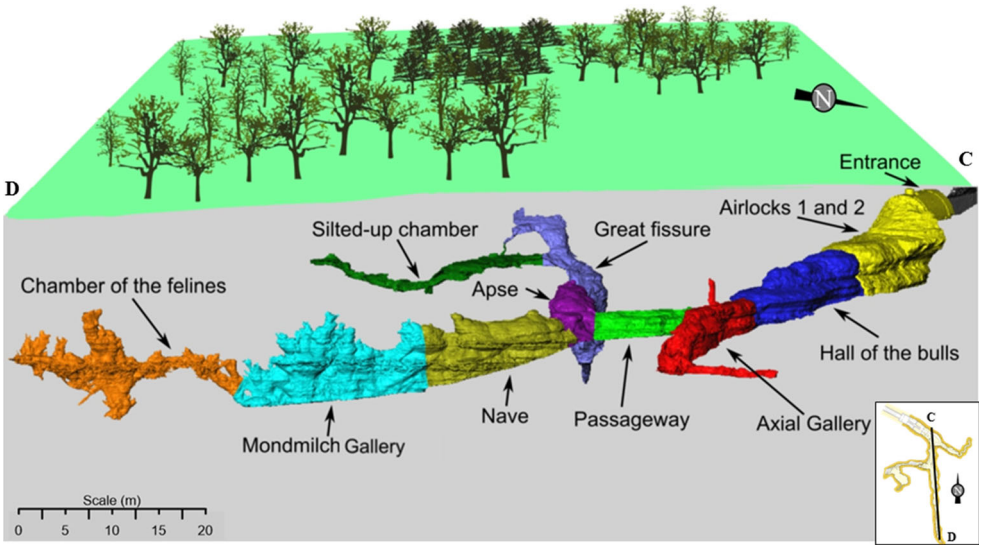

Fig. 3 3D representation of the Lascaux Cave in its environment with location of the different rooms

the Mondmilch Gallery and the Chamber of the Felines. The conduit's dead end is much more confined. It is isolated from the other part of the cave by a natural siphon which makes the access difficult.

The Great Fissure starts from the west of the Apse which is isolated by a hatch and a cover. The Shaft of the Sorcerer, accessible by a ladder, is 5 ms below the Apse. It represents the lower part of the Great Fissure. A scree closes the dead end, 5 m lower. From there, the Great Fissure spans 30 m in the west and goes back to within 5 m below surface. Several roots creeping in this zone emphasizes its closeness to the surface. The silted-up chamber is connected to this fracture for about a 3-m-long and 1-m-wide corridor. This cave zone is largely filled by sandy clay sediments, extended by a winding umbilical conduit. The study focused on the two first parts of the cave: the axial one and the right one.

Methods: monitoring facilities and data analysis

Meteorological and microclimatological monitoring facilities

In Lascaux site, the external atmosphere monitoring system is composed of a weather station located above the cave entrance. Every minute, this weather station records the external atmosphere, soil temperature, relative humidity, wind speed and direction, atmospheric pressure and rainfall rate and intensity.

In addition, an experimental zone was set up with four boreholes. These boreholes are positioned near the cave to determine the carbon dioxide dynamics in the epikarst. An in situ Vaisala IR CO_2 sensors (GMP 221, 0.01% precision) are installed to record every minute the CO_2 partial pressure (PCO_2) at 1, 2, 3 and 8 m depth in the boreholes FC1, FC2, FC3 and FC4, respectively (Fig. 1). Air samples were also grabbed in these four boreholes to measure the $\delta^{13}C_{CO_2}$.

During previous years, a complete monitoring system is installed in Lascaux Cave. The location of the sensors in the cave is presented in Fig. 2. More than 200 sensors are installed to measure various environmental parameters (air and rock temperature, atmospheric pressure, PCO_2, PO_2 and spring discharge). All the PCO_2 values are measured with the calibrated Vaisala IR CO_2 sensors (GMP 221, precision of ±0.2% of the measure, sensitivity of ±0.001%). Carbon dioxide measurements at temperatures and pressures different from the calibration conditions were needed to be corrected. The required compensation for any nondispersive infrared (NDIR) sensor is based on the ideal gas law. The correction for a percent volume reading can be done using Eq. 1, according to the ideal gas law:

$$PCO_{2corrected} = PCO_{2measured} * \left(\frac{1013 * (T + 273)}{289 * P}\right) \quad (1)$$

With PCO_2 in % or ppm, T the temperature in °C and P the atmospheric pressure in hPa. Where 1% of PCO_2 is equivalent to 10,000 ppm.

The temperature measurements are performed by PT100 sensors located in the air and the rocks (precision of ±0.3 °C). The calibration and the wedging inter-probes allow reaching a sensitivity measurement of 0.001 °C. Atmospheric pressures are measured in two points inside the cave using Vaisala sensors (precision and sensitivity of ±0.1 hPa). The epikarstic emergence flow rate is derived from the water level evolution in the collector recorded every minute using a water level sensor.

The measurements made by all these sensors inside and outside the cavity are recorded every minute through AMR

WinControl (Akrobit®) software, especially developed for the data acquisition with the Almenodataloggers (Alhborn®).

Grab air samples were performed in glass bottles in the different parts of the cave and the four epikarstic boreholes. This is to analyze the $\delta^{13}C_{CO_2}$ and determine the CO_2 origins and the mixing ratio with the external atmosphere (Peyraube et al. 2016). The samples were sent to the LAB/ISO (BRGM) and analyzed with a gas chromatography coupled with a mass spectrometer (Gas Bench with Delta +XP; reproducibility of 0.03‰).

The different data series of the microclimatological parameters were analyzed first independently and statistically. The highlighted information is then combined to characterize the air movements taking into account the cave geomorphology. The data analysis was based on the calculation and the comparison of the air densities between the different parts of the cave and the external atmosphere using the approach of Garcia-Anton et al. (2014).

Geochemical monitoring of the epikarstic emergence (SAS1 spring)

Water samples were collected from the epikarstic emergence in the cave weekly from January 2015 to July 2015 (flowing period). Limited access to the cave explains the lack of data during some periods of sampling. Temperature, electrical conductivity, dissolved oxygen and pH were measured in situ using a WTW model 3430 equipped with sentix 950 probe (precision: 0.004 for pH, ±0.3 °C for temperature), tetracon 925 probe (precision: 0.5% of the measure) and FDO 925 probe (precision: 1.5% of the measure). Bicarbonate concentration was measured at the time of sampling by digital titration using 1.6 N H_2SO_4 with a HACH alkalinity meter (precision: 2.44 mg/L). Water samples were collected in 60-mL HDPE bottles and were kept refrigerated until the analysis. Cation samples were preserved with nitric acid. Major element concentrations were measured using the Dionex Models ICS 1500 and ICS 1100 ion chromatography at the Institute of Mechanics and Engineering. The analysis indicated that for the major ions, the charge balance errors of all water samples are of <5%.

Calcite saturation indices (SIcalcite), the CO_2 partial pressure at equilibrium with the atmosphere (PCO_{2eq}) and the CO_2 partial pressure at saturation (Peyraube et al. 2012; Minvielle et al. 2015) with respect to the calcite (PCO_{2sat}) were calculated using PHREEQC (Parkhurst and Appelo 1999). Determination of the calco-carbonic equilibriums of the epikarstic flows allows making a hypothesis for the simulations of the exfiltration water chemical equilibrium at the walls of Lascaux Cave.

Simulations for water equilibrium at walls

Water chemical equilibrium at the walls is involved in calcium carbonate dissolution and precipitation. Two conceptual schemes of these physicochemical processes are presented in Fig. 4a, b.

To quantify the potential effect of condensation and exfiltration waters at the walls, simulation on the behavior of these two types of water with a calcite support in a similar atmosphere of the cave (variable PCO_2) using PHREEQC was employed. These simulations were performed considering that there is a liter of water in a square meter of calcite support. The geochemistry of the condensation water is assumed as being similar to that of non-mineralized water having a low PCO_{2eq} before it reaches equilibrium with the air PCO_2. The exfiltration water was taken as similar to the collected ones at the end of the flow cycle of the epikarstic emergence. To transcribe exfiltration geochemistry in the Hall of the Bulls, this water is considered with a SIcalcite = 0. For this purpose, the concentrations of pH, bicarbonate and calcium ions were adjusted. The values for the two types of simulations are presented in Table 1.

Evaporation processes are assumed to be negligible in Lascaux Cave because of its stable relative humidity values ranging from 99 to 100%. Equation 2 was used to calculate the mass of calcite dissolved or precipitated by a liter of water and by a square meter of calcite support (m_{CaCO_3} in g m^{-2} L^{-1}). These estimations are based on the difference of calcium ion concentration between the initial and the final state of the water (SIcalcite = 0).

$$m_{CaCO_3} = \frac{\left(\left[Ca^{2+}\right]_i - \left[Ca^{2+}\right]_f\right) * M_{CaCO_3}}{S_c} = \frac{\Delta\left[Ca^{2+}\right] * M_{CaCO_3}}{S_c} \quad (2)$$

With $\Delta[Ca^{2+}]$ the difference between$[Ca^{2+}]_i$ and $[Ca^{2+}]_f$, the initial and final calcium concentrations determined through PHREEQC in the aqueous solutions (mol L^{-1}) (condensation or exfiltration waters), M_{CaCO_3} the molar mass of the calcium carbonate (g mol^{-1}) and S_c the contact surface between water and calcium carbonate (m^2).

For the dissolution case, the use of temperature differences air/rock allows to determine the thermal gradient between these two phases. The greater the temperature gradient between air and rock is, the greater the condensation is likely to occur on the wall. For the same relative humidity (near 100% in the cave), the absolute humidity of the mass of the warmer air will be higher than that of the coldest. Moisture excess in the warmer air mass will be compensated by the condensation on the colder wall. It is then possible to approximate, at a moment, the potential

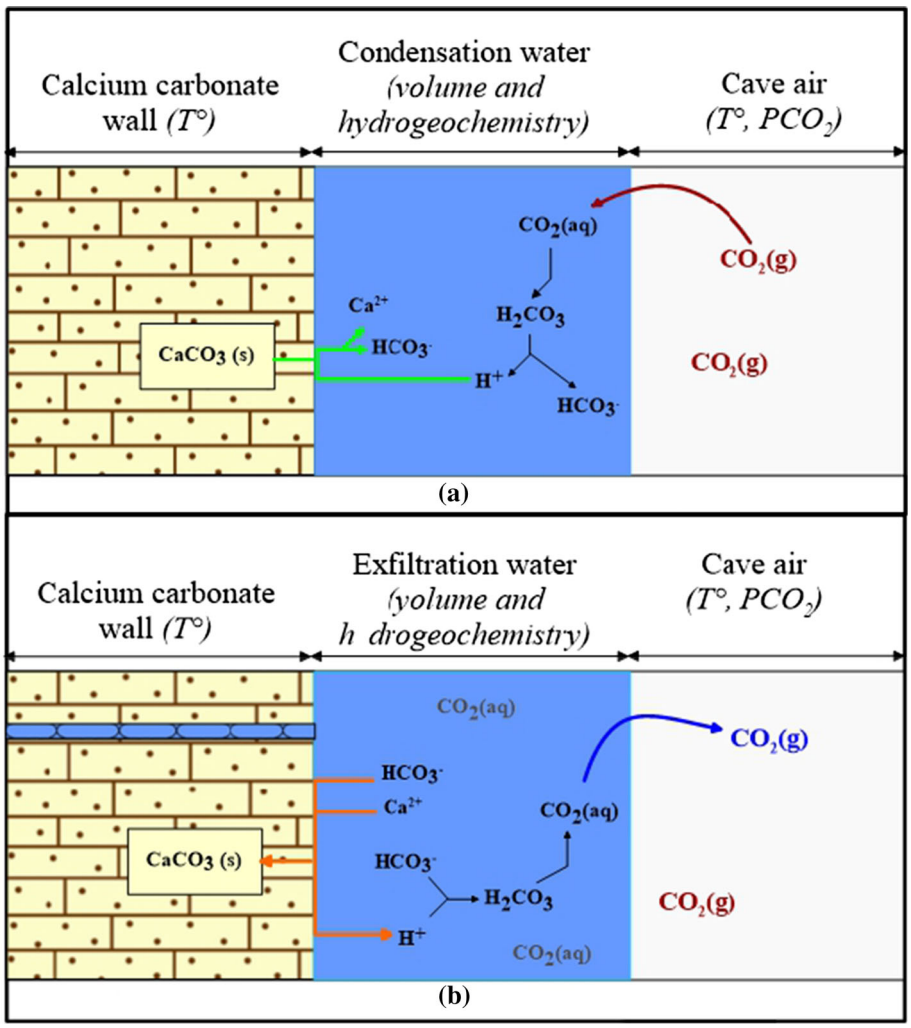

Fig. 4 Two conceptual schemes of calcium carbonate **a** dissolution and **b** precipitation processes. The main parameters (wall and air temperatures, water volume and hydrogeochemistry and air PCO_2) driving these two processes are written in *italics*. Water exfiltration through the stratigraphic boundary is shown (**b**). Chemical reactions are also presented

Table 1 Inputs for the condensation and the exfiltration chemical simulations on the walls

Types of simulation/inputs	Cave atmosphere inputs		Water geochemistry inputs				
	Temperature (°C)	PCO_2 cave air (%)	pH	$[HCO_3^-]$ (mg/L)	$[Ca^{2+}]$ (mg/L)	SIcalcite	PCO_{2sat} (%)
Condensation on the wall	12.6	0–5	5.3	0	0	0	PCO_2 cave air
Exfiltration on the wall	12.6	0–5	7.3	440	150	0	3 and 5

Only the major inputs are presented in this table

volume of condensation water at a particular wall (V_w in L) with Eq. 3:

$$V_w = m_a * (H_a - H_r) = V_a * \rho_a * (H_a - H_r) \quad (3)$$

With m_a the humid air mass (kg), H_a and H_r, the absolute humidity of the air and the air in the rock (kg of water kg^{-1} of humid air), respectively, V_w the water volume (L), V_a the air volume (m^3) and ρ_a the air density (kg m^{-3}). The absolute humidity (H) is obtained using Eq. 4:

$$H = \frac{M_{H_2O}}{M_a} * \left(\frac{e'_w}{P - e'_w}\right) \quad (4)$$

With M_{H_2O} the molar mass of water (g mol^{-1}), Ma the molar mass of the dry air (g mol^{-1}), e'_w the saturated water vapor pressure (Pa) and P the atmospheric pressure (Pa). The saturated water vapor pressure is calculated with Eq. 5 considering θ the temperature (°C) and the empirical coefficients coming from the Smithsonian Meteorological tables:

$$e'_w = 610,78 * \exp\left(\frac{17.08085 * \theta}{234.175 + \theta}\right) \quad (5)$$

The exfiltration water volume at a moment is estimated using in situ observations (wall surface affected and water

film thickness). This volume is considered to be constant and equal to 0.5 L along the year. It is then possible to estimate the potentially dissolved or precipitated mass of calcium carbonate for a particular wall (m'_{CaCO_3} in g) considering the water volume (V_w) with Eq. 6:

$$m'_{CaCO_3} = m_{CaCO_3} * V_w \quad (6)$$

To simplify the method, numerical relations were determined between the PCO_2 of the air and the mass of calcium concern (condensation or exfiltration) without performing simulations systematically through PHREEQC software. It is as if air PCO_2 and calcium carbonate mass affected by dissolution and precipitation are linked by the chemical relations depending on temperature. The assumption is that the temperature effects are low because of the stability of this parameter in the cave (0.5 °C of variation during the study period) as demonstrated by Minvielle (2015). These relationships give, at a moment, an estimation of the potentially dissolved and precipitated mass of calcium carbonate on the walls, taking into account the PCO_2 values in Lascaux Cave. Each calculation is made supposing that the values of PCO_2 and temperature remain constant. Kinetics of the reactions (precipitation and dissolution) is not taken into account. This limitation is due to the logistical impossibility of physical measurements on the wall: at present, it is not possible to measure condensation water thickness and its evolution on the wall. In addition, it is not yet possible to know with accuracy which surface on the wall is affected by condensation. However, the total amount of condensation water on the wall can be estimated. Results, then, will be provided in grams for a wall. No annual amount of dissolved or precipitated calcite will be calculated.

Finally, to apply these simulations and outputs to a particular point of the cave (Hall of the Bulls), the volumes of condensation and exfiltration were used to weigh the masses of calcite potentially dissolved and precipitated.

Results

Cave time series data

Atmosphere and cave climatology

The meteorological time series data at the exterior of the cavity of Lascaux (Table 2) during the study period are coherent with the local standard climate normal recorded from the French Meteorological Organization. These data present the normal seasonal weather pattern in the Southwest France having a typical continental influences (cold in winter and warm in summer). However, 2015 is the warmest recorded year in Lascaux site since the 1950s (beginning of the meteorological measures). The atmospheric temperature is in the average of 12.94 °C from February 2015 to February 2016. During this period, external minimum and maximum temperature is of −4.5 and 40.7 °C, respectively.

Figure 5 presents the epikarstic spring's (a) discharge and rainfall, (b) the density differences between the external atmosphere and cave air, (c) the barometric pressure, (d) the cave air temperature and (d) PCO_2 data series in the cave. The total rainfall during the study period reached 670 mm which is 23.9% lower than the normal (Lopez 2009). Epikarstic discharge (183 m^3) is 49.2% lower than the last 10 year average (372 m^3). Water flow is recorded from February to July 2015 with two principal flood events on the 25th and 29th of February 2015 (6 and 8 m^3/day). Epikarstic flow resumed in January 2016 with a flood event on the 12th of January (14 m^3/day). The density differences between external atmosphere and cave air were positive from February to May 2015 and from November 2015 to February 2016. Exchanges might have happened between the cave and external atmosphere during these periods. Barometric pressure shows typical evolution with highest variation (±40 hPa) during winter storms and late summer thunderstorms.

Temperature in the different parts of the cave was stable through time. However, it varied with respect to depth. The lowest (10.492 °C in March 2015) and highest (14.034 °C in October 2015) temperatures were recorded in the SAS1 near the entrance of the cave (Table 2). In the adorned parts of the cave, the maximum (12.936 °C in December 2015) and the minimum values (12.383 °C in July 2015) of temperature were recorded in the Hall of the Bulls. However, the average maximum values during the study period were seen in the Apse (12.690 °C) and the minimum in the Axial Gallery (12.524 °C). This area represents the cold point of the adorned part of the cave. These observations can be explained by the geomorphology of the cave. In fact, the Axial Gallery corresponds to a cold air trap. Seasonal variations are recorded. It showed that the range of variation decreased with depth (minimum in the Axial Gallery and the Mondmilch Gallery). This information highlights the influence of the thermal conduction throughout the calcarenite massif on the cave temperature. Indeed, the cave is located in the heterothermic zone of the massif because of its shallow depth. This mechanism is consistent with the previous study of Lacanette et al. (2007). This research shows that the temperature of the rock surrounding the cave followed a classic trend and influenced the air temperature. This phenomenon brought the inversion of the thermal gradient in the cave from April 2015 to August 2015 (Fig. 5d) because of the delay of the thermal wave arrivals with respect to depth.

Table 2 Average, maximum and minimum values of temperature (Temp), barometric pressure (BP) and PCO_2 values from February 2015 to February 2016

Location/sensor	Study Average	Maximum	Minimum
Meteorological station			
Temp (°C)	12.937	40.700	−4.500
BP (hPa)	997.4	1018.2	971.2
Epikarstic boreholes			
CO_2 1 m (%)	2.141	3.807	0.621
CO_2 2 m (%)	3.434	5.277	2.172
CO_2 3 m (%)	4.353	5.150	3.436
CO_2 8 m (%)	4.837	5.817	2.728
Cave (SAS1)			
Temp (°C)	12.659	14.034	10.492
CO_2 (%)	1.670	2.435	0.654
Cave (Hall of the Bulls)			
Temp (°C)	12.639	12.936	12.383
CO_2 (%)	1.736	2.571	1.094
Cave (Axial Gallery)			
Temp (°C)	12.524	12.925	12.488
CO_2 (%)	1.800	2.941	1.525
Cave (Passageway)			
Temp (°C)	12.590	12.824	12.498
CO_2 (%)	2.233	3.231	1.320
Cave (Apse)			
Temp (°C)	12.690	12.932	12.568
CO_2 (%)	2.372	3.817	1.401
BP (hPa)	999.3	1020.2	973.3
Cave (Mondmilch Gallery)			
Temp (°C)	12.631	12.695	12.591
CO_2 (%)	2.819	3.715	2.092
Cave (Chamber of the Felines)			
Temp (°C)	12.624	12.796	12.541
CO_2 (%)	2.944	3.627	2.138

During this period, the temperature was lower in the Hall of the Bulls than in the deep parts of the cavity.

PCO_2 and $\delta^{13}C_{CO_2}$ in the cave

The different cave PCO_2 values are presented in Fig. 5e. Minimum was recorded in January 2016 (0.65%) in the SAS and maximum in February 2015 (3.817%) in the Apse.

PCO_2 decreased from February 2015 to June 2016 and then increased for the rest of the period. High-PCO_2 conditions were recorded from July 2015 to February 2016. Two different trends were observed in the adorned parts of the cave. The first was in the deep part (Mondmilch Gallery and the Chamber of the Felines) and the other in the shallow part of the cave (Hall of the Bulls, Axial Gallery, Passageway and Apse).

In the shallow parts, highest PCO_2 were recorded in winter (February 2015 to April 2015) and autumn (September 2015 to February 2016) reaching 3.2% in February 2015. PCO_2 values were different in the four zones, increasing with depth. Barometric pressure and flood events seem to influence the PCO_2 measures. However, it is impossible to dissociate the influence of these two environmental parameters because of low pressure accompanied by rainfall leading to a flood event. During the warm season (April to August 2015), PCO_2 values were lower than in winter. PCO_2 levels were similar in the four different zones (1.5–1.7%). Barometric pressure seems to have low effect on PCO_2. In the deep parts, the PCO_2 were similar in the two zones (Mondmilch Gallery and Chamber of the Felines). These PCO_2 values vary from 2.1 to 3.7%, maximum in February 2015 and minimum in May and June 2015.

In addition, grab samples were collected in the different parts of the cave in order to perform the analysis of the $\delta^{13}C_{CO_2}$. Results show depleted values in all the zones (Table 3). Values range from −22.7‰ in the shallow parts

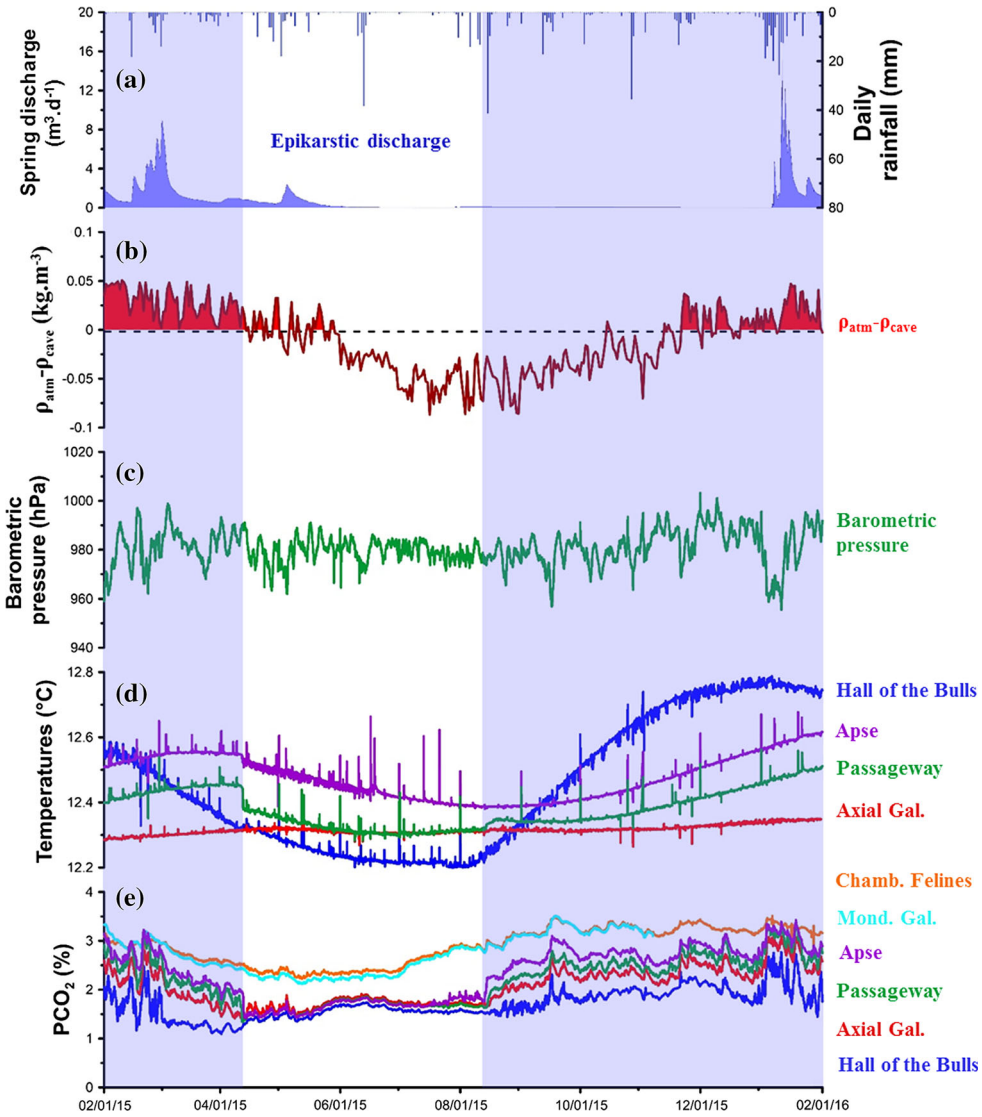

Fig. 5 Meteorological and PCO_2 time series inside the Lascaux Cave from February 2015 to February 2016. Epikarstic emergence flow rate and daily rainfall (**a**), differences of the air density between atmosphere and cave (**b**) (*shaded in red* indicates potential exchanges between atmosphere and cave) and the atmospheric pressure (**c**) are presented. Temperatures (**d**) and PCO_2 (**e**) measurements allow the determination of two different aerologic regimes inside the cave (*gray and white fonts*). The peaks observed on the temperature curves result from human entrance in the cave

(Hall of the Bulls) to −23.6‰ in the deep parts (Mondmilch Gallery).

Epikarst time series data

PCO_2 and $\delta^{13}C_{CO_2}$ in the epikarst

CO_2 concentrations in the epikarst ranged from 0.60 to 5.80% and increased with depth: 2.1, 3.4, 4.4 and 4.8% on the average for FC1, FC2, FC3 and FC4, respectively (Fig. 6). The seasonal variations are pronounced in FC1 and FC2. This could be explained by CO_2 production by the biosphere and the exchanges with the external atmosphere. The isotopic analysis of the $\delta^{13}C_{CO_2}$ made in the four boreholes showed a biogenic origin and a more depleted CO_2 at 3 and 8 ms because of the lower influence of the external atmosphere with depth. Values of the $\delta^{13}C_{CO_2}$ range from: −21.4‰ at 8 m deep to −24.7‰ at 3 m deep (Table 3). Maximum and minimum PCO_2 values were observed in May 2015 and during the winter 2015, respectively. In FC3, PCO_2

Table 3 $\delta^{13}C_{CO_2}$ (‰) values measured in the epikarstic boreholes and in the different rooms of the Lascaux the 05/04/2015

Location/points	Date	$\delta^{13}C_{CO_2}$ (‰)
Epikarstic boreholes		
FC1 (1 m)	05/04/2015	−22.3
FC2 (2 m)		−22.5
FC3 (3 m)		−24.7
FC4 (8 m)		−21.4
Cave		
Hall of the Bulls	05/04/2015	−22.7
Axial Gallery		−22.8
Apse		−22.9
Mondmilch Gallery		−23.6

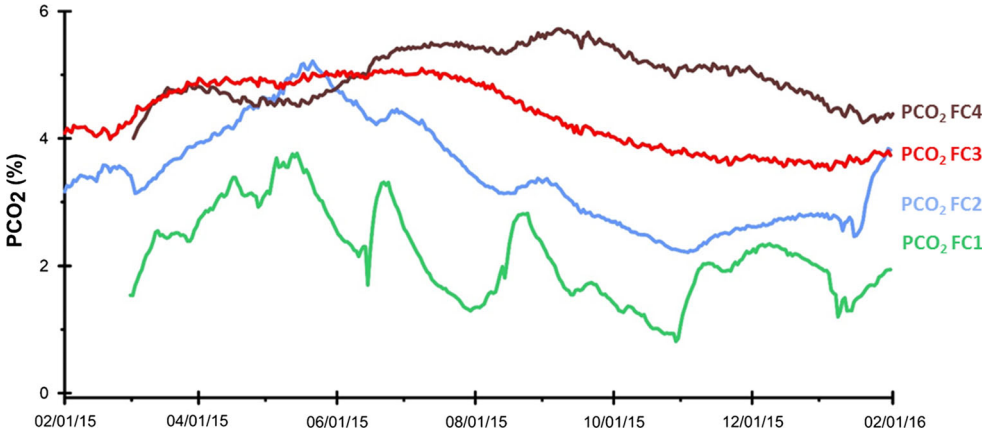

Fig. 6 PCO_2 time series recorded in the four boreholes FC1, FC2, FC3 and FC4, respectively, at 1, 2, 3 and 8 m of depth, from February 2015 to February 2016

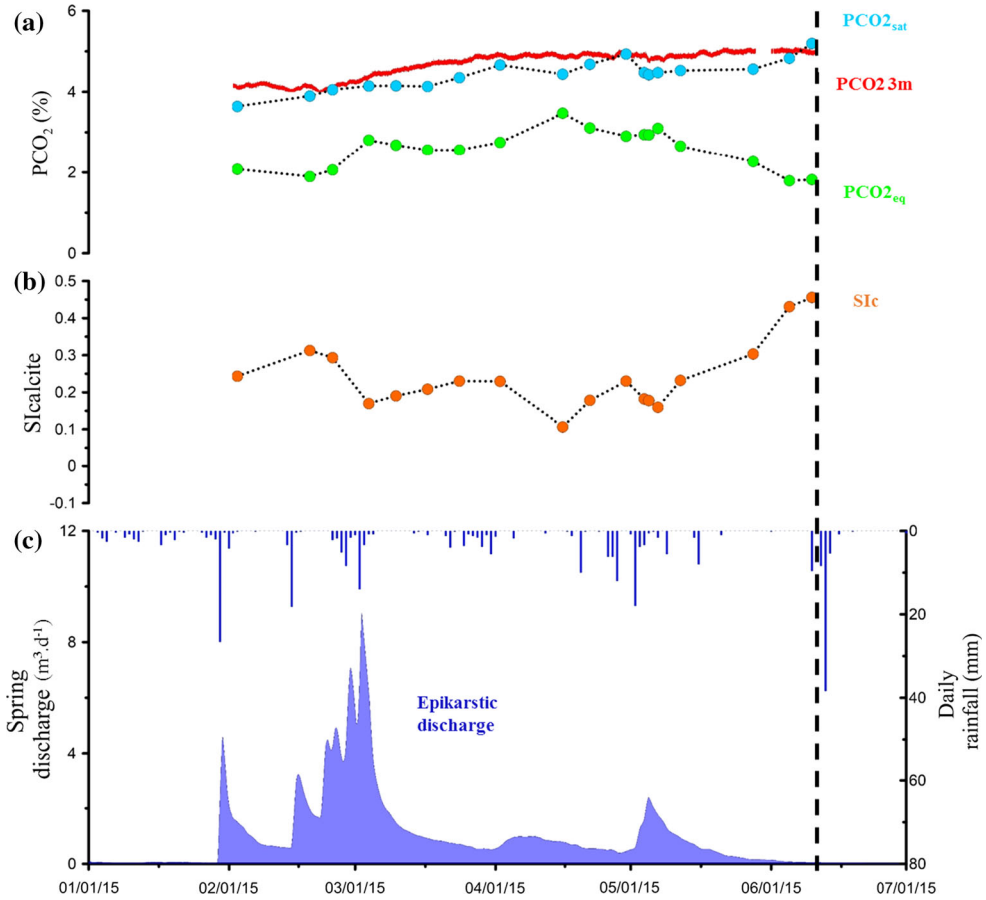

Fig. 7 Evolution of equilibrium and saturation values of PCO_2 (**a**) and of the SIcalcite (**b**) from water of the epikarstic emergence of Lascaux Cave for the discharge period of 2015. Discharge, daily rainfalls (**c**) and epikarstic air PCO_2 at 3 m depth (**a**) are also shown. The *dash bar* represents the end of the flow at the epikarstic emergence

are more stable with 3.4% in winter 2015 for minimum values and 5.15% for maximum in June 2015. The measurement in the deep zone (FC4) reached higher PCO_2 during summer. It showed less pronounced seasonal variability than in the shallower boreholes.

Geochemistry of the epikarstic emergence

PCO_2 recorded in the epikarstic boreholes at 3 m deep (FC3), water PCO_{2eq} and water PCO_{2sat} are presented in Fig. 7 (a) SIcalcite, (b) the epikarstic flow rate and (c) the daily rainfall are also shown.

Water is mostly supersaturated with regard to the calcite (SIcalcite > 0.1) having PCO_{2eq} from 1.5 to 3.0%. The epikarstic flows coming into the cave are supersaturated with respect to the calcite which means that the water will degas CO_2 and potentially precipitate calcite on its arrival in the cave. PCO_{2sat} values vary from 3.5 to 5% and increase during the flow period. Maximum value of 5% was recorded after the last flood event in June 2015. The

PCO_{2sat} are consistent with PCO_2 values of the epikarstic atmosphere ranging from 4 to 5% during the flowing period.

Simulations of condensation and exfiltration waters equilibrium on the walls

The different simulation inputs are based on the information (cave, epikarst and epikarstic flow geochemistry) gathered from the different monitoring devices. First, evolution of condensation water (1 L m^{-2}) on a calcium carbonate wall under different theoretical conditions (different air PCO_2) was simulated. Consequently, behavior of exfiltration on a calcite wall (1 L m^{-2}) coming from the epikarst was also simulated. Exfiltration water at equilibrium with respect to calcite with PCO_{2sat} of 3% (PCO_2 in the deep parts of the cave) and 5% according to the epikarstic emergence PCO_{2sat} (epikarst PCO_2) are considered. Dissolved and precipitated calcium carbonate masses are then calculated. Results are presented in Table 4.

For the condensation, the higher the air PCO_2 is, the higher the mass of dissolved calcium carbonate is. For an air PCO_2 of 0.1 and 3.0%, the dissolved calcite masses are 0.09 and 0.37 g L^{-1} m^{-2}, respectively. For the exfiltration water, simulations have shown that the higher the difference between the air PCO_2 and the water PCO_{2sat} is, the higher the precipitation of calcium carbonate is. Calcite precipitation ranges from 0 g L^{-1} m^{-2} when the water PCO_{2sat} and the air PCO_2 are equal to 0.28 g L^{-1} m^{-2} with the PCO_{2sat} of 5.00% and air PCO_2 of 0.1%.

Different relationships between air PCO_2 and masses of calcium carbonate dissolved or precipitated can be considered (Fig. 8). A power regression is proposed to estimate the mass dissolution of calcite (Eq. 7). Two regressions permit to estimate directly the calcium carbonate precipitation considering only the air PCO_2 and the initial PCO_{2sat} of water (Eqs. 8 and 9, respectively, for water initial PCO_{2sat} of 3 and 5%). Coefficients of determination are found close to 0.99. These regression equations are assumed to be valid only for the air PCO_2 values used for the previous simulations.

$$m\mathrm{CaCO_{3dissolved}} = \left(0.204 * \mathrm{PCO_2^{0.359}}\right) \quad (7)$$

$$m\mathrm{CaCO_{3precipitated}} = -0.01 * \mathrm{PCO_2^3} + 0.065 * \mathrm{PCO_2^2} - 0.182 * \mathrm{PCO_2} + 0.225 \quad (8)$$

$$m\mathrm{CaCO_{3precipitated}} = -0.004 * \mathrm{PCO_2^3} + 0.039 * \mathrm{PCO_2^2} - 0.156 * \mathrm{PCO_2} + 0.287 \quad (9)$$

The estimation of the mass of calcium carbonate dissolved or precipitated for a particular wall (m'_{CaCO_3} in g) can be performed considering the potential volume (V_w) of condensation and exfiltration waters. These relationships will be used in the next part to estimate at a moment, the potential masses of calcium carbonate affected by condensation and exfiltration on the left wall of the Hall of the Bulls.

Discussion

The dynamics of the cave internal aerology

Lascaux Cave as a study site is interesting specifically when looking on the air exchanges between the cavity and the external atmosphere. There are a lot of concerns in this adorned cave that makes this site particular.

Actually, Lascaux Cave is isolated from the external atmosphere through the two airlock doors (SASs) which serve as buffer to prevent the direct exchanges of the cavity to the exterior. These SAS doors are designed to produce thermal insulation from the scree initially present at the entrance of the cavity. The air temperature measurements conducted in the different parts of the cavity confirm its isolation from the external atmosphere (Fig. 5). The values

Table 4 Dissolution and precipitation of mass of calcium carbonates ($m\mathrm{CaCO_3}$) on the wall for a contact surface of 1 square meter and an aqueous solution volume of 1 L

Air PCO_2 (%)	$m\mathrm{CaCO_3}$ (g L^{-1} m^{-2}) dissolved by condensation	$m\mathrm{CaCO_3}$ (g L^{-1} m^{-2}) precipitated by exfiltration (Initial PCO_{2sat} = 3.00%)	$m\mathrm{CaCO_3}$ (g L^{-1} m^{-2}) precipitated by exfiltration (Initial PCO_{2sat} = 5.00%)
0.1	0.09	0.21	0.28
0.5	0.16	0.14	0.21
1	0.20	0.10	0.16
1.5	0.23	0.07	0.13
2	0.26	0.04	0.10
2.5	0.28	0.02	0.08
3	0.30	0	0.06
4	0.34		0.04
5	0.37		0

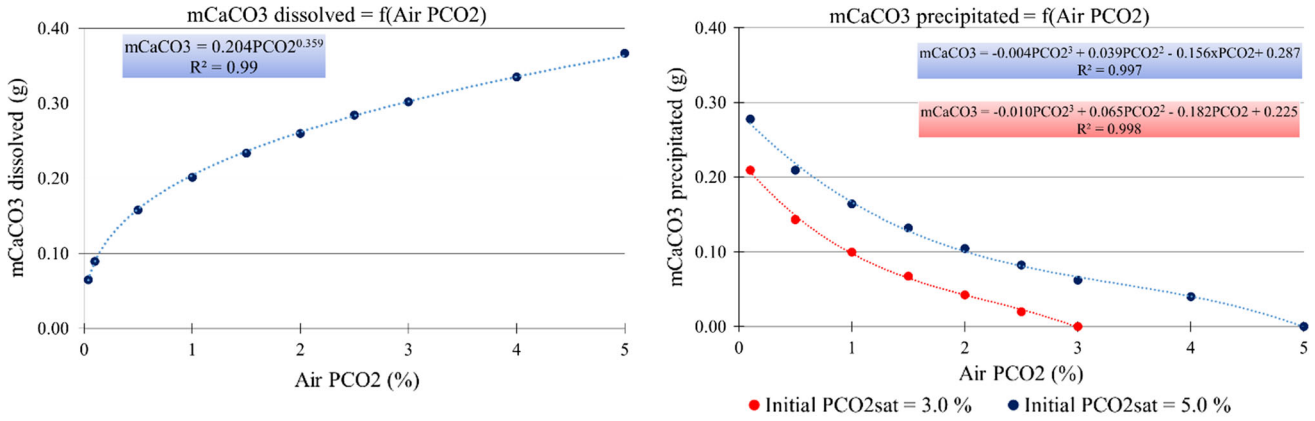

Fig. 8 Relationships between air PCO_2 and mass of dissolved calcite for condensation water (*left*) or mass of precipitated calcite for exfiltration water (*right*)

obtained from the air temperature were stable and correlated to the rock temperature. Figure 9 presents the difference in between the rock and calculated air temperature for the following parts of the cavity: (a) Hall of the Bulls, (b) Axial Gallery, (c) Passageway, (d) Apse, (e) Nave and (f) Mondmilch Gallery. The temperature difference between the rocks and the air was at the maximum value of 0.08 °C at the left wall of the Hall of Bulls. This is with exception of the infrequent human influence which can contribute warmth and humidity (risk of having condensation). The temperature difference was low (less than 0.01 °C) in the following zones of the cavity: Passageway, Apse and Nave. It is even lower or negligible at the Axial Gallery and the Mondmilch Gallery. Hence, the temperature is directly constrained by the thermal conduction in the underlying massif calcarenite. The PCO_2 in the cavity remained high (more than 1.09% in the adorned parts) all throughout the year (Fig. 5). This is even during the time when the density difference of the external air and the air on the cavity gave rise to draining the cave air, having a PCO_2 decrease. The daily variations are due to the variations of the atmospheric pressure as demonstrated by Denis (2005). Moreover, the isotopic $\delta^{13}C_{CO_2}$ values are depleted in all areas of the cavity, confirming that the participation of the enriched external air (−9.6‰, NOAA 2016) is low in terms of the composition of the cave atmosphere.

Although the cavity is confined, measured PCO_2 levels in the different zones present significant concentration variations within the year (more than 1.0% in the different parts of the cave). As a consequence, two different cave air conditions or regimes were observed in the cavity (based on the PCO_2 data and the air temperature). There are two identified regimes: stratification and convection. Period is used as a division of the whole duration (one year) of the study period. This gives the following division: (Period 1) stratification from 01/02/2015 to 10/04/2015; and (Period 2) convection from 10/04/2015 to 11/08/2015; and (Period 3) another stratification from 11/08/2015 to 01/02/2016. Stratification is characterized by different and stable air masses affected by the air movement that are negligible. Convection, on the other hand, shows the presence of homogenous air masses influenced by air movements allowing communication to several cavity zones. Figure 10 shows the consequences of these two cave air conditions or regimes in the distribution of the PCO_2 in the cavity (Inverse Distance Weight interpolation).

The first period is observed when the thermal gradient inside the cavity is inversely correlated to depth. The warmest zones in the cavity are the shallowest room (e.g., Hall of the Bulls). The recorded PCO_2 values are then different in each measured zone; these have the tendency to increase with respect to depth (Fig. 5e). This observation is important in terms of considering the factors of stratification in the atmosphere. The increase in CO_2 concentration with respect to depth brought also an augmentation of the air mass volume with the depth. High air density was observed at the deep zones. The observed variations (±1.0%) at the beginning of this period are associated with the variations of the atmospheric pressure and the flow at the epikarstic emergence. This means that air mass is not the same in all the cavity zones.

The second period was observed in the cavity from the month of April 2015. It occurred when the air temperature in the Hall of the Bulls (shallow zone) became lesser than the deep zones. This inverse thermal gradient took place due to the conduction effect of the cold thermal wave (external winter temperature) through the overlying massif (Lacanette and Malaurent 2010). The cold air coming from the Hall of the Bulls is also recorded in the temperature station points of Passageway and Apse. This activity corresponds to setting up of the convection cells. It homogenizes the different air masses present in the Hall of the

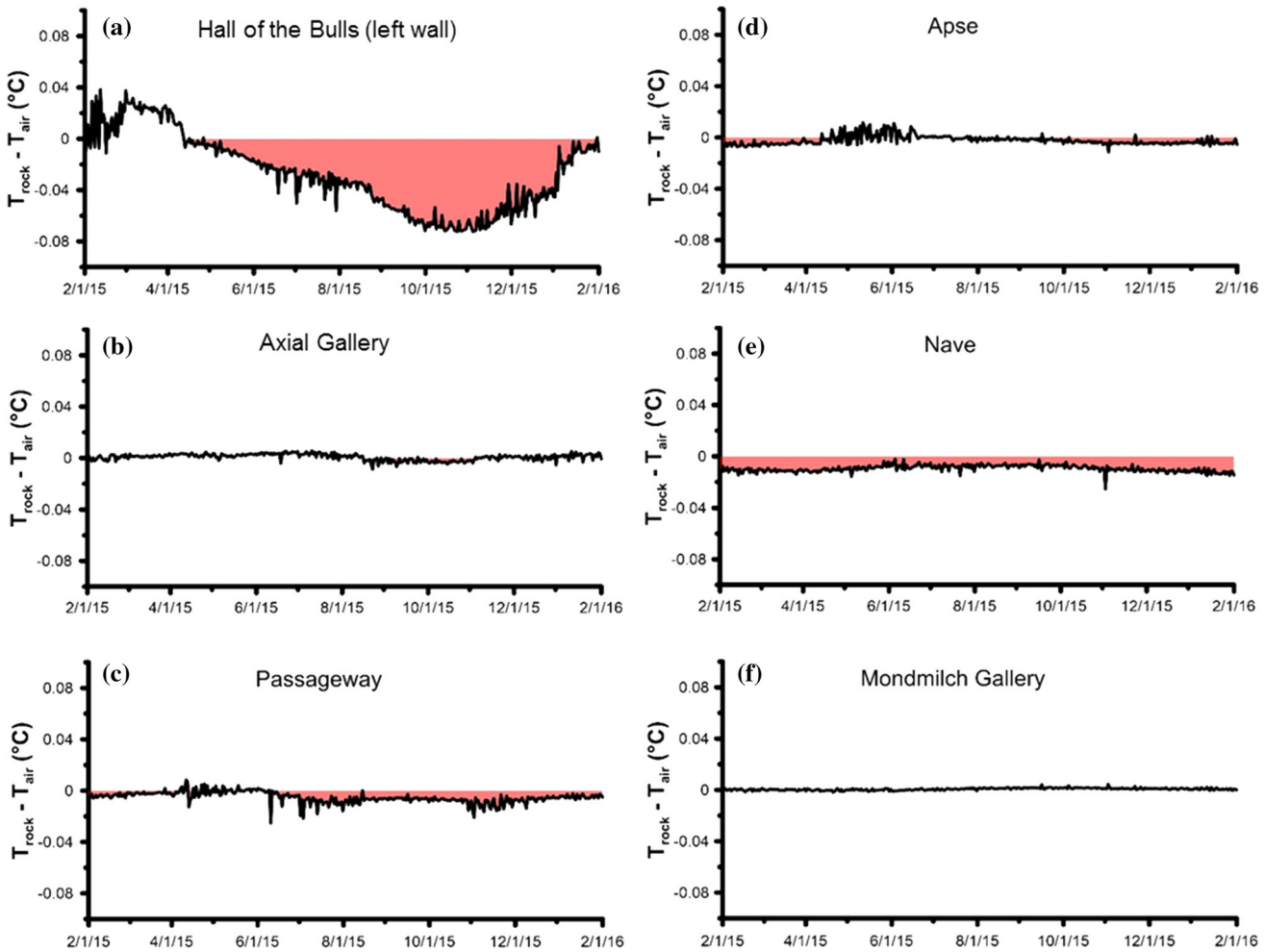

Fig. 9 Evolution of temperature differences between the rock and the air in the Hall of the Bulls (**a**), the Axial Gallery (**b**), the Passageway (**c**), the Apse (**d**), the Nave (**e**) and the Mondmilch Gallery (**f**) from February 2015 to February 2016. The *red shades* show the potential periods of condensation at the wall (Trock-Tair < 0.0 °C). The *peaks* are due to imbalances caused by human entrance in the cavity and the advective movements resulting from changes in atmospheric pressure

Bulls, Axial Gallery, Passageway, as well as in the Apse as shown by similar PCO_2 values recorded in the different zones (Fig. 5e). Since the setup of the convection cells, it is observed that the measured PCO_2 in the Axial Gallery, Passageway and Apse decreased but not in the Hall of Bulls. This signifies that the CO_2 levels, after placing the convection cell, is a result of the CO_2 levels from different zones brought about by the volume differences in each of the zones. The CO_2 levels in the Hall of the Bulls increased due to high CO_2 contribution of the deep zones influenced by convection. The Mondmilch Gallery and the Chamber of the Felines were not affected by the convection cells because of their morphology. Also higher CO_2 levels were observed in these zones than in the shallow ones. It was noticed in all zones that the variations in the atmospheric pressure have less impact on measured PCO_2, contrary to the previous stratification period. This confirms the fact that the two homogenous air masses form in the cavity from April to middle August 2015, one in the deep zones and the other in the most superficial areas.

Toward end of August until the rest of the study period, the stratification regime was replaced. The PCO_2 signals in the different zones of the cavity dissociated. An atmospheric condition similar to the first period was observed, i.e., PCO_2 that increases with depth. Also atmospheric pressure variation and water flow in the epikarst have greater influence on PCO_2 than during the convection period.

The distinction in between the two cave air conditions allowed having a better understanding of the air mass movement, hence, the distribution of the PCO_2 in the cavity of Lascaux. Furthermore, this permitted to distinguish the periods and the cavity zones where the risk of dissolution of adorned walls through condensation is the highest. In terms of microclimatic conditions, the more problematic areas are the zones of the cavity in which air

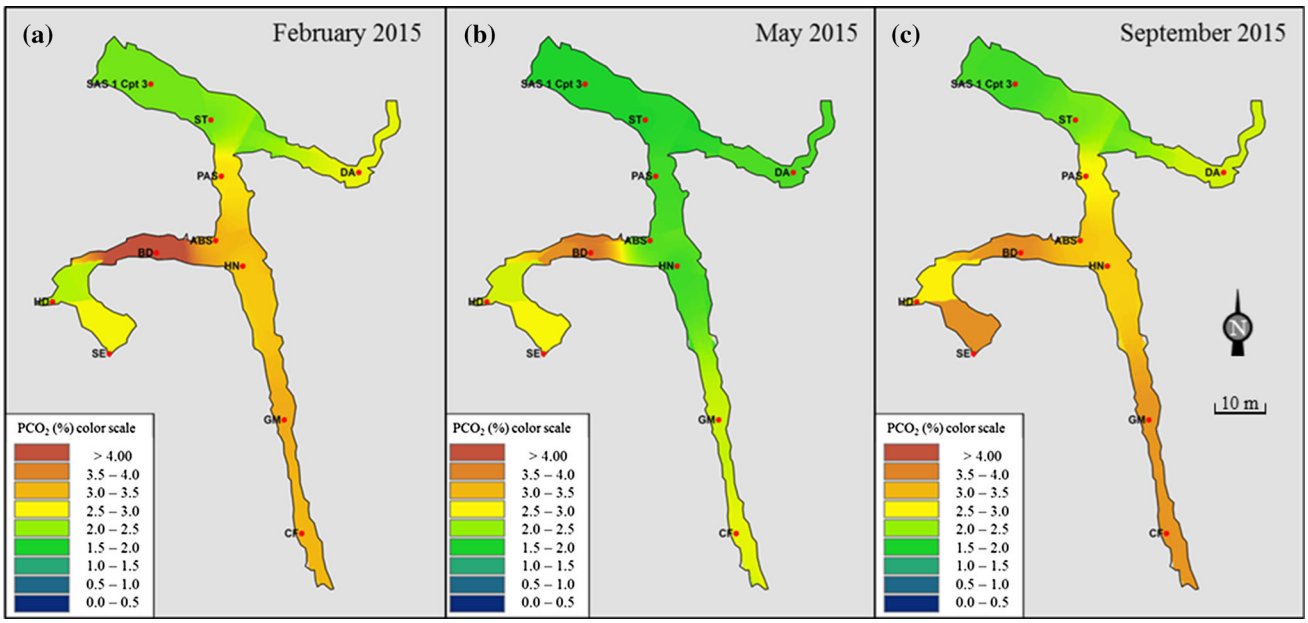

Fig. 10 Spatial distribution of the partial pressures of CO_2 in Lascaux Cave (Inverse Distance Weight interpolation) for the three different periods (stratification: **a** and **c**; convection: **b**). Data for each contour map correspond to average monthly measurements calculated using PCO_2 values recorded every minute by the 11 sensors (locations on the contour maps)

will be stratified. During the period of stratification, environmental disturbance will be localized in a small zone of the cavity. On the other hand, during the period of convection, the air movement distributes its effect in a larger volume.

Potential calcium carbonate evolution on the wall of the Lascaux Cave: importance of the dynamics of the cave internal aerology

In this section, the left wall of the Hall of the Bulls was used as an example to illustrate the application of the method used. It is in this most adorned zone of the cavity that the exfiltration and the condensation water are potentially the most considerable as given evidence by the evolution of the temperature differences between air and rock (Fig. 8a). The first step consists of determining the water volume from exfiltration and the condensation potentially present on the wall at time t. The water volume from exfiltration present at time t in this wall was estimated from the maximum surface of the wall affected by exfiltration during this year (around 10 m^2) and the observed thickness of the water layer settled in the cavity (50 µm). This volume is considered constant throughout the year. In this example, the considered water volume from exfiltration is 0.5 L. To estimate the water volume from the potential condensation, it was considered that the excess moisture content in the whole air volume in the Hall of the Bulls (400 m^3) would condense on the left wall. From Eq. 3, the calculated water volume that can condense on the left wall of the Hall of the Bulls progressed from 0 to 0.02 L during the study period. It is assumed that when the potential condensation is equal to 0, the dissolution process cannot take place on the wall.

To estimate the calcite mass, potentially dissolved or precipitated, on the wall, the determined relationships (Eqs. 7, 8 and 9) were used to obtain an approximation of the dissolved or precipitated calcite mass value on a weekly basis. The average PCO_2 weekly values of the measured air were taken into consideration as well as the potential water volume of the condensation and exfiltration present on the wall. The results obtained are presented in Fig. 11. In this figure, the evolution of the calcite mass, potentially (a) precipitated by the exfiltration under two scenarios (PCO_{2sat} of 3 and 5%), or (b) dissolved by condensation water on the wall is shown. The exfiltration period and the potential condensation period on the left wall of the Hall of the Bulls obtained from the (c) temperature difference between air and rock are also portrayed. The evolution of the PCO_2 values used for the simulation is showed. It is important to note that this figure does not give a temporal assessment of the affected mass calcite on the wall. Rather, it provides the potential mass of the dissolved or precipitated calcite under the conditions of the PCO_2 and temperature. For example, for an air PCO_2 at 3% and a condensation volume of 0.02 L, the potential dissolution of the calcite through water condensation of about 0.006 g for all the left wall of the Hall of the Bulls can be expected.

The exfiltration on the left wall of the Hall of the Bulls was observed from April 2015 until February 2016. The

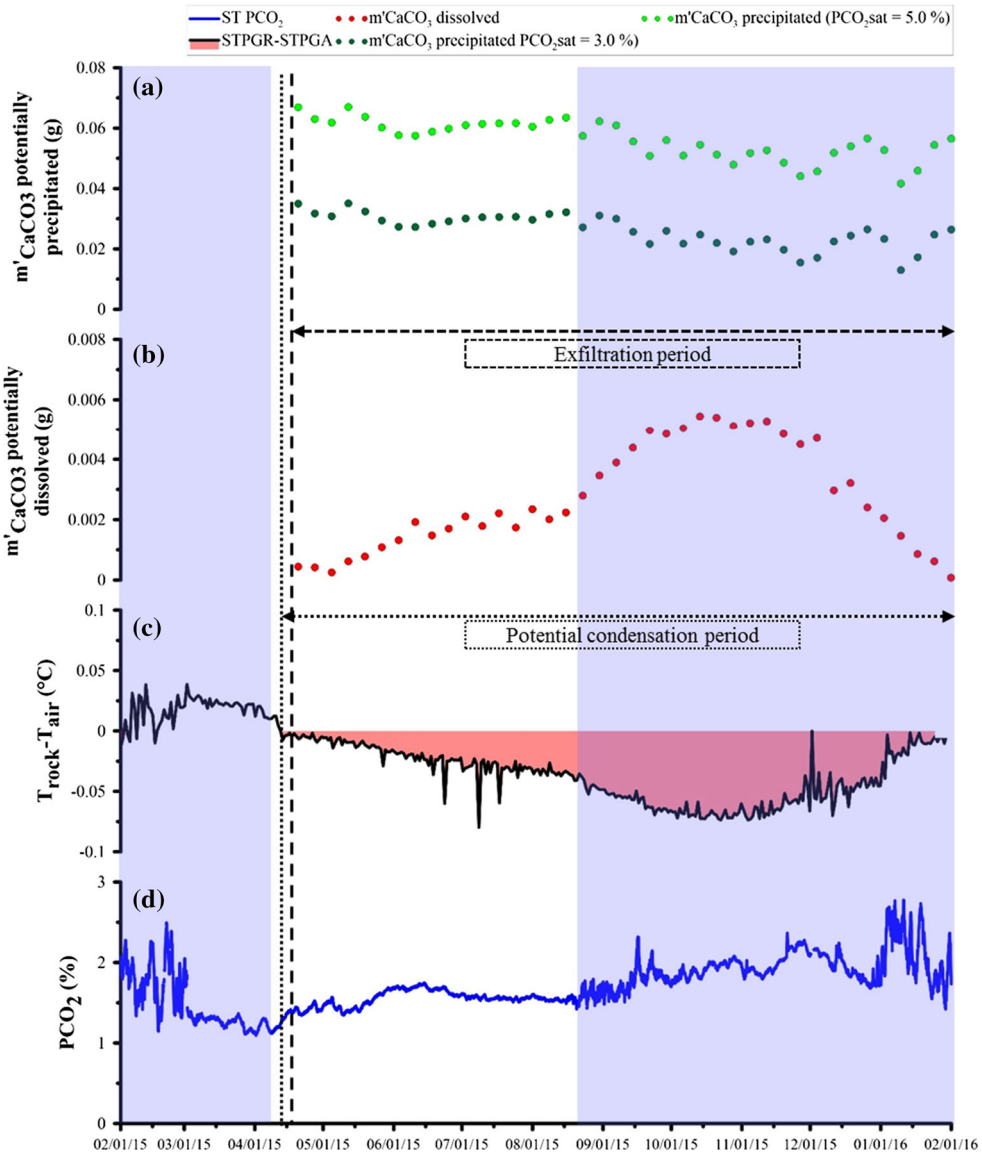

Fig. 11 Weekly estimation of the mass of calcium carbonate potentially precipitated (**a**) and dissolved (**b**) at the left wall of the Hall of the Bulls taking into account the air PCO_2 values recorded in this room (**d**) and the estimation of the condensation and exfiltration water volume. In addition, temperature differences between rock and air at the left wall of the Hall of the Bulls (**c**) are presented to determine the potential condensation periods (the *point line* represents the beginning of the condensation period). *Dash line* represents the beginning of the exfiltration. *Gray* and *white* backgrounds represent, respectively, stratification and convection processes period in the Lascaux Cave

estimation of the calcite mass potentially precipitated varied from 0.013 to 0.036 g and 0.042 to 0.068 g for water having PCO_{2sat} initial at 3 and 5%, respectively. Thus, the greater the difference between the PCO_2 of the air and the initial PCO_{2sat}, the greater the potential precipitation can be expected. This implies that the temporal distribution of the air PCO_2 in the Hall of the Bulls plays an important role in the precipitation process of the calcite on the adorned wall. This precipitation phenomenon could consequently, in the long term, become problematic if the conservation of the paintings on the wall is a concern.

The potential condensation period on the left wall of the Hall of the Bulls started during the time when convection was present (April 2015). Convection between the Hall of the Bulls and the deep and warmest zones brought the temperature in the Hall of the Bulls to increase. The left wall was not in thermal equilibrium with air that could potentially allow condensation on the support. The condensation was then possible on this support until February 2016 with an increased risk during the second period of stratification (August 2015 to December 2015). The temperature gradient between air and the rock on the left wall of the Hall of the Bulls was restricted by the internal aerologic conditions of the cavity. During the potential period of condensation, the calcite mass that is potentially dissolved varied from 0.0002 to 0.0051 g with the values lesser than those of April 2015 and at the same time higher than those of winter 2015–2016. It denotes that the affected calcite mass is less important in the dissolution case than that of precipitation. Nevertheless, the dissolution is still important in terms of cavity conservation if the condensed water is renewed on the wall. However, no drips from condensation were observed on the left wall of the Hall of the Bull, even for the period where the condensation was

most probable to occur (highest air and rock temperature difference). It also seems coherent that the condensed water on the surface of the wall will be in equilibrium with the air temperature. This could mean that the condensation will not be renewed unless there will be a perturbation, e.g., human entry. Moreover, it is noteworthy that the exfiltration period on the left wall of the Hall of the Bulls coincides with the potential period of condensation. It can then be considered that the dissolution of the calcite through condensation will be less to negligible on the surface of the wall affected by the exfiltration. So from the precipitation to the support, exfiltration will immediately buffer the condensation in these zones.

The cave air condition, therefore, is important when considering the risks of dissolution and precipitation of the walls of a karst cavity. The dynamics of the cave air or its internal aerology is the origin of the distribution of the CO_2 levels in the cavity. It is also responsible for the disequilibrium of the temperature between air and rock that can produce condensation, consequently, dissolution on the wall. In addition, this will influence the re-equilibration processes of the natural system after being perturbed and its potential consequences. For instance, entry of human on the cavity creates thermal disequilibrium (contributing heat) and hydric stress (contributes water vapor) that could cause condensation on the wall. This disequilibrium will be distributed in the volume of the cavity involved in the convection loop at this phase (lesser risk), whereas, it will be concentrated in a smaller volume during the stratification phase (higher risk) as shown by Lacanette and Malaurent (2010). The internal aerology of the cavity should, therefore, be considered by the cave manager to anticipate and avoid the potential disorders brought by human entry.

Implication of the proposed method to cave management

The data series acquired from February 2015 to February 2016 showed that there is no considerable and direct influence of external atmosphere on the internal aerology of Lascaux Cave. The security SAS doors obstruct the direct exchanges with the external atmosphere. This makes the cavity of Lascaux distinct in terms of cave air condition: high CO_2 concentration throughout the year (0.6–3.9%). The air temperature of the cave is constrained by the rock temperature, influenced per se by the thermal conduction through the calcarenite massif. Even if the values of the microclimatic parameters are stable, it is observed that the internal aerology of the cavity is dynamic. This is as two internal aerologic regimes (stratification and convection) were able to determine. These regimes constrain the distribution of the air masses, hence, the air PCO_2 in the cavity throughout the year. The air cavity was stratified from February 2015 to April 2015. In this period, the air masses are distinct, varying in terms of spatiotemporal pattern with increasing PCO_2 with respect to depth. Convection then took place from the beginning of August 2015 after the inverse temperature gradient with respect to depth. Similar PCO_2 values were observed in the zones affected by the convective cells. In general, values are smaller with the exception at the Hall of the Bulls. Finally, there was the reoccurrence of the stratification in the cavity until February 2016.

Geochemical simulations (using PHREEQC software) were used to study the influence of cave internal aerology on calcite precipitation and dissolution. Dissolution may be caused by condensation, and precipitation may be caused by exfiltration present on the walls. The simulations allowed determining three relationships connected to the mass of the calcium carbonate influenced by dissolution and precipitation as a function of air PCO_2 in the cavity. These relationships led to estimating a potential calcite mass either dissolved or precipitated in a weekly basis using the measured PCO_2 data. The obtained relationships and results were then applied to the left wall of the Hall of Bulls. The results showed small amount of dissolved calcite mass. Nevertheless, it indicates that the calcite can be affected by condensation with the presence of the atmosphere that is loaded with CO_2 like in the case of the Hall of the Bulls. The calcite mass potentially precipitated through exfiltration is more important. It is influenced by the air PCO_2 and its geochemistry.

From the application, the results, however, can still be developed. This is as in this case, no monitoring of mass calcite was done due to logistic constraints. As of the moment, it is impossible to determine the flow of condensation and exfiltration in the stratigraphic boundary. Furthermore, the simulations conducted considered a pure support of calcite which is not the real case of the cavity of Lascaux as it is constituted of Coniacian calcarenite. This gives a result of an overestimated dissolved calcite mass which can eventually pose problems in terms of information for conservation measures. The approach can be improved by considering simulations of the support that is closer to reality and determining more precisely the hydrogeochemical signal of the water from exfiltration and water condensation (PCO_{2sat}, SIcalcite, etc.).

Nonetheless, this research shows that the internal aerology of a karst cavity, i.e., Lascaux, plays a major role in the spatiotemporal distribution of the temperature as well as CO_2 concentration. The latter influences the precipitation and dissolution of calcite. The dynamics of the internal aerology of this cavity isolated from the exterior is essential in studying the actual and past evolution of the speleothems in similar cavities. It is also vital, in terms of

conservation issues. For instance, using a high-resolution monitoring and high-frequency parameters such as microclimate and PCO_2 is helpful in determining more precisely the possible spatiotemporal distribution of the air PCO_2 in the cave. For these reasons, taking into consideration all these information in managing the cavity can facilitate in anticipating the potential natural perturbations (e.g., changes in climate) or in any consequences that a human entry can bring.

Conclusion

This research aims to determine the dynamics of the internal aerology of a subsurface karst cavity using high-frequency monitoring of PCO_2 and high-resolution microclimatic parameters measurements. Understanding the internal aerology of the cavity allowed disclosing the responsible mechanisms of the internal dynamics of the CO_2 in the adorned cave of Lascaux (Montignac, France). The spatiotemporal distribution of the PCO_2 is then taken into consideration to estimate the calcite mass possibly affected by the condensation and exfiltration waters on the left wall of the Hall of the Bulls, the most overseen zone as this contains most of the recognized prehistoric paintings.

CO_2 and temperature measurements showed that there are two aerologic regimes: stratification and convection. Stratification gives different values of CO_2 with respect to depth. It occurs from September to April when air thermal gradient is inversely correlated to the depth of the cave. Convection gives a homogenous value of CO_2 in the cave. It occurs from April to August when the shallow parts of the cave are colder than the deep parts. CO_2 levels in cave air have an effect on the water in the cave, triggering water to precipitate or dissolve the carbonate.

In order to calculate the potential calcite variations caused by precipitation or dissolution, a method using PHREEQ C is proposed. The method relies on the identification of the condensation and exfiltration periods taking into account CO_2 levels and water volumes on the wall. Each calculation is made considering all parameters constant. Kinetic aspects are not considered. Values of calcite potential variation are given in grams for the whole wall. The result showed that for Lascaux, during the study period (February 2015 February 2016), the potential of calcite precipitation is higher than the potential of dissolution. Calcite potential precipitation ranged from 0.013 to 0.068 g. Calcite potential dissolution ranged from 0.0002 to 0.0051 g.

This serves as an evidence that the proposed method allows determining which calcite evolution process (e.g., dissolution or precipitation) is potentially predominant for the wall with respect to the considered period and conditions (PCO_2, temperature differences between air and rock). Consideration of all of the obtained information is important to cave management. It can facilitate in anticipating the potential natural perturbations (e.g., changes in climate) or in any consequences that a human entry can bring.

Acknowledgements The authors would like to thank the DRAC Aquitaine, Poitou-Charentes and Limousin for funding and supporting this research.

References

Atkinson TC (1977) Carbon dioxide in the atmosphere of the unsaturated zone: an important control of ground-water hardness in limestone. J Hydrol 35:111–123

Aujoulat N (2004) Lascaux. Le geste, l'espace et le temps. Seuil, Paris. Collection. Arts rupestres, 274 p, ill. en couleur, pp 271–272

Baldini JU, Baldini LM, McDermott F, Clipson N (2006) Carbon dioxide sources, sinks, and spatial variability in shallow temperate zone caves: evidence from Ballynamintra Cave, Ireland. J Cave Karst Stud 68:4–11

Batiot C (2002) Etude expérimentale du cycle du carbone en régions karstiques. Apport du carbone organique et du carbone minéral à la connaissance hydrogéologique des systèmes. Site expérimental de Vaucluse, Jura, Larzac, Région Nord-Montpelliéraine, Nerja (Espagne). Thèse de Doctorat, Univ. D'Avignon, 247 p

Batiot-Guilhe C, Seidel J-L, Jourde H, Hébrard O, Bailly-Comte V (2007) Seasonal variations of CO_2 and 222 Rn in a Mediterranean sinkhole-spring (Causse d'Aumelas, SE France). Int J Speleol 36:51–56

Benavente J, Vadillo I, Carrasco F, Soler A, Liñán C, Moral F (2010) Air carbon dioxide contents in the vadose zone of a Mediterranean karst. Vadose Zone J 9:126. doi:10.2136/vzj2009.0027

Bourges F, Genthon P, Mangin A, D'Hulst D (2006) Microclimates of l'Aven d'Orgnac and other French limestone caves (Chauvet, Esparros, Marsoulas). Int J Climatol 26:1651–1670. doi:10.1002/joc.1327

Bourges F, Genthon P, Genty D, Mangin A, D'Hulst D (2012) Comment on "Carbon uptake by karsts in the Houzhai Basin, southwest China" by Junhua Yan et al. J Geophys Res Biogeosci. doi:10.1029/2012JG001937

Breecker DO (2017) Atmospheric pCO2 control on speleothem stable carbon isotope compositions. Earth and Planet Sci Lett 458:58–68

Cigna A (2002) Monitoring of caves: conclusions and recommendations. Acta Carsologica 31:175–177

Cuezva S, Fernandez-Cortes A, Benavente D, Serrano-Ortiz P, Kowalski AS, Sanchez-Moral S (2011) Short-term CO_2(g) exchange between a shallow karstic cavity and the external atmosphere during summer: role of the surface soil layer. Atmos Environ 45:1418–1427. doi:10.1016/j.atmosenv.2010.12.023

Delluc B, Delluc G (2006) Connaître Lascaux. Editions du Sud-Ouest, 77 p

Denis A (2005) Identification of functional relationships between atmospheric pressure and CO_2 in the cave of Lascaux using the concept of entropy of curves. Geophys Res Lett. doi:10.1029/2004GL022226

Dreybrodt W, Scholz D (2011) Climatic dependence of stable carbon and oxygen isotope signals recorded in speleothems: from soil

water to speleothem calcite. Geochim Cosmochim Acta 75:734–752. doi:10.1016/j.gca.2010.11.002

Ek C (1981) Mesures du CO_2 dans l'air des grottes: comparaison Québec-Belgique. In: International Union of Speleology (ed) 8th international congress of speleology, Bowling Green (Kentucky). International Union of Speleology, pp 672–673

Ek C, Gewelt M (1985) Carbon dioxide in cave atmospheres. New results in Belgium and comparison with some other countries. Earth Surf Process Landf 10:173–187

Fernandez PL, Gutierrez I, Quindos LS, Soto J, Villar E (1986) Natural ventilation of the paintings room in the altamira cave. Nature 321:586–587

Fernandez-Cortes A, Cuezva S, Garcia-Anton E, Alvarez-Gallego M, Pla C, Benavente D, Cañaveras JC, Calaforra JM, Mattey DP, Sanchez-Moral S (2015) Changes in the storage and sink of carbon dioxide in subsurface atmospheres controlled by climate-driven processes: the case of the Ojo Guareña karst system. Environ Earth Sci 74:7715–7730. doi:10.1007/s12665-015-4710-2

Garcia-Anton E, Cuezva S, Fernandez-Cortes A, Benavente D, Sanchez-Moral S (2014) Main drivers of diffusive and advective processes of CO_2-gas exchange between a shallow vadose zone and the atmosphere. Int J Greenh Gas Control 21:113–129. doi:10.1016/j.ijggc.2013.12.006

James JM (1977) Carbon dioxide in cave atmosphere. Trans Br Cave Res Assoc 4:417–429

Kaufmann G, Dreybrodt W (2007) Calcite dissolution kinetics in the system $CaCO_3$-H_2O-CO_2 at high undersaturation. Geochim Cosmochim Acta 71:1398–1410

Kowalczk A (2009) High resolution microclimate study of Hollow Ridge Cave: Relationships between cave meteorology, air chemistry, and hydrology and the impact on speleothem deposition. Thesis, Florida State University

Kowalczk AJ, Froelich PN (2010) Cave air ventilation and CO_2 outgassing by radon-222 modeling: how fast do caves breathe? Earth Planet Sci Lett 289:209–219. doi:10.1016/j.epsl.2009.11.010

Kowalski AS, Serrano-Ortiz P, Janssens IA, Sanchez-Moral S, Cuezva S, Domingo F, Were A, Alados-Arboledas L (2008) Can flux tower research neglect geochemical CO_2 exchange? Agric For Meteorol 148:1045–1054

Kuzyakov Y (2006) Sources of CO_2 efflux from soil and review of partitioningmethods. Soil Biol Biochem 38:425–448

Lacanette D, Malaurent P (2010) La 3D au service de la conservation des grottes ornées, l'exemple de Lascaux et du simulateur Lascaux. In Situ. doi:10.4000/insitu.6793

Lacanette D, Malaurent P, Caltagirone J-P, Brunet J (2007) Étude des transferts de masse et de chaleur dans la grotte de Lascaux: le suivi climatique et le simulateur. Karstologia 50:19–30

Liñán C, Vadillo I, Carrasco F (2008) Carbon dioxide concentration in air within the Nerja Cave (Malaga, Andalusia, Spain). Int J Speleol 37:2

Lopez B (2009) Les processus de transfert d'eau et de dioxyde de carbone dans l'épikarst: Aide à la conservation par le développement de nouvelles méthodologies pour l'étude de l'environnement des cavités. Application à la Grotte de Lascaux (Montignac, France). Thèse de Doctorat, UniversitéDe Bordeaux 1, 384 p

Mangin A, Bourges F, D'Hulst D (1999) Painted caves conservation: a stability problem in a natural system (the example of the prehistoric cave of Gargas, French Pyrenees). C R Acad Sci Paris 328:295–301

McDonough LK, Iverach CP, Beckmann S, Manefield M, Rau GC, Baker A, Kelly BFJ (2016) Spatial variability of cave-air carbon dioxide and methane concentrations and isotopic compositions in a semi-arid karst environment. Environ Earth Sci 75(8):1–20

Milanolo S, Gabrovšek F (2009) Analysis of carbon dioxide variations in the atmosphere of Srednja Bijambarska Cave, Bosnia and Herzegovina. Bound Layer Meteorol 131:479–493. doi:10.1007/s10546-0

Minvielle S (2015) Etude de l'infiltration et de ses variations interannuelles en contexte épikarstique pour la caractérisation du fonctionnement des hydrosystèmes karstiques : utilisation de la méthode ISc-PCO_2 et des modèles réservoirs. Thèse de Doctorat, Université de Bordeaux, 302 p

Minvielle S, Peyraube N, Lastennet R, Denis A (2015) Characterization of the functionality of karstic systems based on the study of the SIc–Pco2 relation. In: Andreo B, Carrasco F, Durán JJ, Jiménez P, LaMoreaux JW (eds) Hydrogeological and environmental investigations in karst systems. Springer, Berlin, pp 19–26

NOAA ESRL Global Monitoring Division (2016) Mace Head site, Ireland. http://www.esrl.noaa.gov/gmd/dv/data/index.php?site=MHD&parameter_name=Carbon%2BDioxide&frequency=Discrete. Accessed 16 Nov 2016

Parkhurst DL, Appelo CAJ (1999) User's guide to PHREEQC (version 2)—a computer program for speciation, batch-reaction, one-dimensional transport, and inverse geochemical calculations: U.S. Geological Survey Water-Resources Investigations Report 99-4259, 312 p

Peyraube N, Lastennet R, Denis A (2012) Geochemical evolution of groundwater in the unsaturated zone of a karstic massif, using the relationship. J Hydrol 430–431:13–24. doi:10.1016/j.jhydrol.2012.01.033

Peyraube N, Lastennet R, Villanueva JD, Houillon N, Malaurent P, Denis A (2016) Effect of diurnal and seasonal temperature variation on Cussac cave ventilation using CO_2 assessment. Theor Appl Climatol. doi:10.1007/s00704-016-1824-8

Renault P (1968) Sur la distinction de plusieurs régions karstiques en raison de la teneur en anhydride carbonique des atmosphères de grottes. C R Acad Sci Paris 267:2288–2290

Scholz D, Mühlinghaus C, Mangini A (2009) Modelling $\delta^{13}C$ and $\delta^{18}O$ in the solution layer on stalagmite surfaces. Geochimica et Cosmochimica Acta 73(9):2592–2602

Spötl C, Fairchild IJ, Tooth AF (2005) Cave air control on dripwater geochemistry, Obir Caves (Austria): implications for speleothem deposition in dynamically ventilated caves. Geochim Cosmochim Acta 69:2451–2468. doi:10.1016/j.gca.2004.12.009

Troester JW, White W (1984) Seasonal fluctuations in the carbon dioxide partial pressure in a cave atmosphere. WRR 20:153–156

Vieten R, Winter A, Warken SF, Schröder-Ritzrau A, Miller TE, Scholz D (2016) Seasonal temperature variations controlling cave ventilation processes in Cueva Larga, Puerto Rico. Int J Speleol 45(3):7

White WB (1988) Geomorphology and hydrology of karst terrains. Oxford University Press, New York

Williams PW (1983) The role of the subcutaneous zone in karst hydrology. J Hydrol 61(1):45–67

Wood WW (1985) Origin of caves and other solution openings in the unsaturated (vadose) zone of carbonate rocks: a model for CO_2 generation. Geology 13:822–824

Wood WW, Petraitis MJ (1984) Origin and distribution of carbon dioxide in the unsaturated zone of the southern high plains. Water Resour Res 20:1193–1208